A design study of mirror modules and an assembly based on the slumped glass for an Athena-like optics

Basso, Stefano, Civitani, Marta, Pareschi, Giovanni, Buratti, Enrico, Eder, Josef, et al.

Stefano Basso, Marta Civitani, Giovanni Pareschi, Enrico Buratti, Josef Eder, Peter Friedrich, Maria Fürmetz, "A design study of mirror modules and an assembly based on the slumped glass for an Athena-like optics," Proc. SPIE 9603, Optics for EUV, X-Ray, and Gamma-Ray Astronomy VII, 96030N (4 September 2015); doi: 10.1117/12.2188509

SPIE.

Event: SPIE Optical Engineering + Applications, 2015, San Diego, California, United States

A design study of mirror modules and an assembly based on the slumped glass for an Athena-like optics.

Stefano Basso*[a], Marta Civitani[a], Giovanni Pareschi[a], Enrico Buratti[a], Josef Eder[b], Peter Friedrich[b], Maria Fürmetz[b],

[a] INAF - Osservatorio Astronomico di Brera (Italy)
[b] Max-Planck-Institut für extraterrestrische Physik (Germany)

ABSTRACT

The Athena mission was selected for the second large-class mission, due for launch in 2028, in ESA's Cosmic Vision program. The current solution for the optics is based on the Silicon Pore Optics (SPO) technology with the goal of $2m^2$ effective area at 1keV (aperture about 3m diameter) with a focal length of 12m. The SPO advantages are the compactness along the axial direction and the high conductivity of the Silicon. Recent development in the fabrication of mirror shells based on the Slumped Glass Optics (SGO) makes this technology an attractive solution for the mirror modules for Athena or similar telescopes. The SGO advantages are a potential high collecting area with a limited vignetting due to the lower shadowing and the aptitude to curve the glass plates up to small radius of curvature. This study shows an alternative mirror design based on SGO technology, tailored for Athena needs. The main challenges are the optimization of the manufacturing technology with respect to the required accuracy and the thermal control of the large surface in conjunction with the low conductivity of the glass. A concept has been elaborated which considers the specific benefits of the SGO technology and provides an efficient thermal control. The output of the study is a preliminary design substantiated by analyses and technological studies. The study proposes interfaces and predicts performances and budgets. It describes also how such a mirror system could be implemented as a modular assembly for X-ray telescope with a large collecting area.

Keywords: glass optics, X-ray optics, Athena, slumped glass, Thin Glass Mirrors, SGO, mirror module, mirror assembly

1. INTRODUCTION

The big collecting area required for the future X-ray telescopes imposes the need to build the X-ray mirror following a modular approach, like in the past has been adopted for visual observatory on ground. Athena[1] will be a pioneer of this class of spacecraft and its challenging angular resolution (<5") leads to big technologic effort to demonstrate the feasibility of light and high performance optics. In the recent years the two main technologies foreseen for Athena, the Silicon Pore Optics[2] (SPO) and Slumped Glass Optics[3][4] (SGO) concentrated their effort in realization of single modules in order to obtain the required performance in term of resolution and feasibility. The collecting area of these modules increases with the years thanks to the improving ability in the integration of the reflecting shells, but they are not yet enough to fulfill the Athena requirements. On the other hand the assembly of all the modules must be also taken into account to demonstrate that the modular concept is feasible. In this paper we focus the attention on the design of the overall assembly considering a SGO technology based on the results obtained in Europe by INAF-Osservatorio Astronomico di Brera (OAB)[5] and Max-Planck-Institut für extraterrestrische Physik (MPE)[6]. In USA the SGO technology developed in a parallel way reaching the capability of assembly an entire telescope for the NuSTAR[7] mission. For Athena the resolution has to be improved by a factor of 10, but the SGO demonstrates its potential ability especially for inner radii of curvature, a region where SPO technology could meet some forming problems.
A special attention has been paid to the thermal control in order to assess the needed power to guarantee a limited optical degradation.
The integration procedure of the single mirror module (MM) makes use of ribs providing the needed stiffness and an integration machine that aligns the glass foils during the curing of the glue[8]. The parabolic and hyperbolic surfaces of

* stefano.basso@brera.inaf.it; fax +39-02-72320496

Optics for EUV, X-Ray, and Gamma-Ray Astronomy VII, edited by Stephen L. O'Dell, Giovanni Pareschi,
Proc. of SPIE Vol. 9603, 96030N · © 2015 SPIE · CCC code: 0277-786X/15/$18 · doi: 10.1117/12.2188509

the Wolter-I configuration are made by two different glass foils and a design of the single module has already been studied[9].

Table 1 - Athena requirements[1][10]

Parameter	*Value*
Focal length	12 m
Effective Area	2 m^2 at 1 keV / 0.25 m^2 at 6 keV
Field of View	40'x40'
Angular resolution (HEW, Half Energy Width)	5" (on axis) / 10" at 25' radius
Mirror Assembly Module (MAM) mass (supporting structure, X-ray baffle, thermal baffle and expandable Sun protection baffle)	1128 kg
Electrical Power	1800 W

Two different types of MM have been considered, one with long optical shells, i.e. 200 mm (par.) + 200 mm (hyp), and one with short optical shells, i.e. 100 mm (par.) + 100 mm (hyp). The advantage of the short configuration is a mass reduction with respect to the long configuration, while on the other hand the short configuration is characterized by more optical shells and it means more time for manufacturing, integration and more costs.
The overall structure, here called also as petal, has been considered in CRFP for a good matching of the thermal expansion with the glass material and for its good space qualification: it is used for example for the eRosita[11] optical bench. Its big dimension (3 m diameter) must be kept in mind thinking about the end to end calibration and even if a single structure is preferable for the mechanical point of view it involves a bigger effort for X-ray tests on ground. An update of the PANTER facility is under study for the accommodation of the whole Athena assembly.
In the next sections the analysis of the mirror assembly and the analysis of the single module are separated. The proposed concept takes the thermal baffle and the X-ray baffle into account as the scheme in Figure 1. The MM mounting proceeds from the detector side, while the thermal baffle is kept independent from the MM and mounted directly on the petal from the space side.

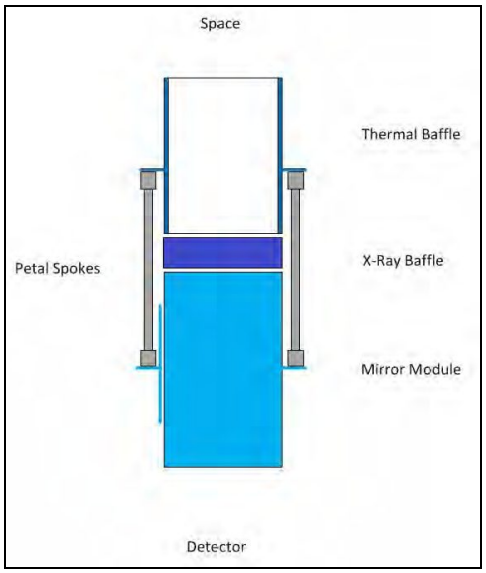

Figure 1 – scheme of the mirror assembly components

2. MIRROR ASSEMBLY

The number of MMs in the assembly depends on different factors as interfaces, the capability of manufacturing them, the calibration concept, etc. The assembly interface points with the spacecraft should be positioned in correspondence of the radial walls to provide stiffness, the azimuthal size of the slumped glassed could be limited by slumping process or by the integration machine: the prototypes developed so far have an azimuthal width of about 200 mm, so this dimension has been considered as reference. The baseline assembly is composed by 138 MMs distributed on 7 rings (ring 1 is the innermost). If the petal is seen from section the shape should be not flat, but curved in order to minimize the optical aberration off-axis (Figure 2) shifting the intersection plane (plane that is the intersection between parabola and hyperbola) toward the focal plane for the outer MMs. This shift is low, less than the petal axial thickness (400 mm), therefore it is not considered in the analysis.

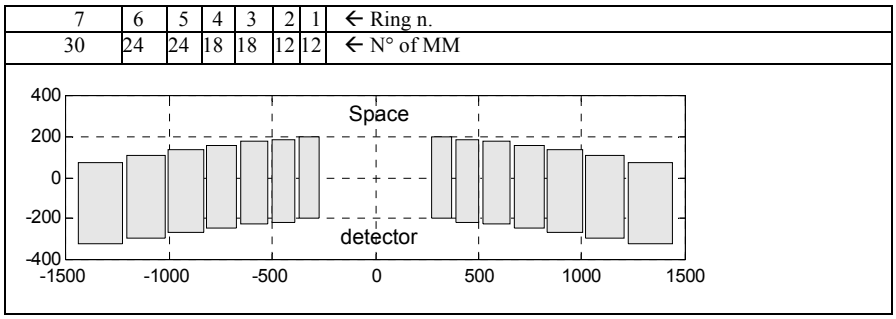

Figure 2 – axial shift and number of MMs

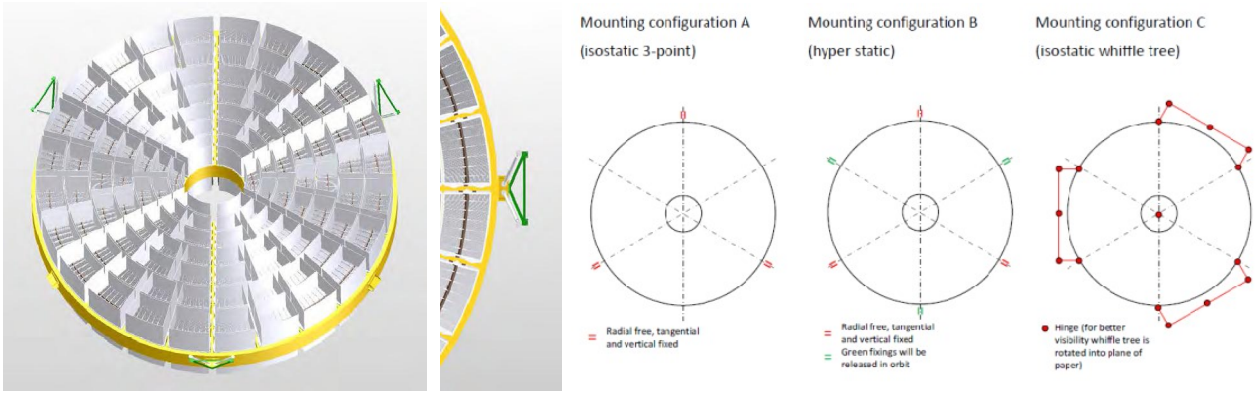

Figure 3 – different types of interfaces: configurations for in-orbit condition (A), during launch (B) and assembling-testing (C)

Different types of interface have been considered (Figure 3).

2.1 FEM DESCRIPTION

The analyses are performed only at primary structure level. The FEM model of the mirror assembly consists of the spoke wheel loaded by concentrated masses at the center of gravity of the mirror modules. The total mass of the proposed CFRP petal is 240 kg.

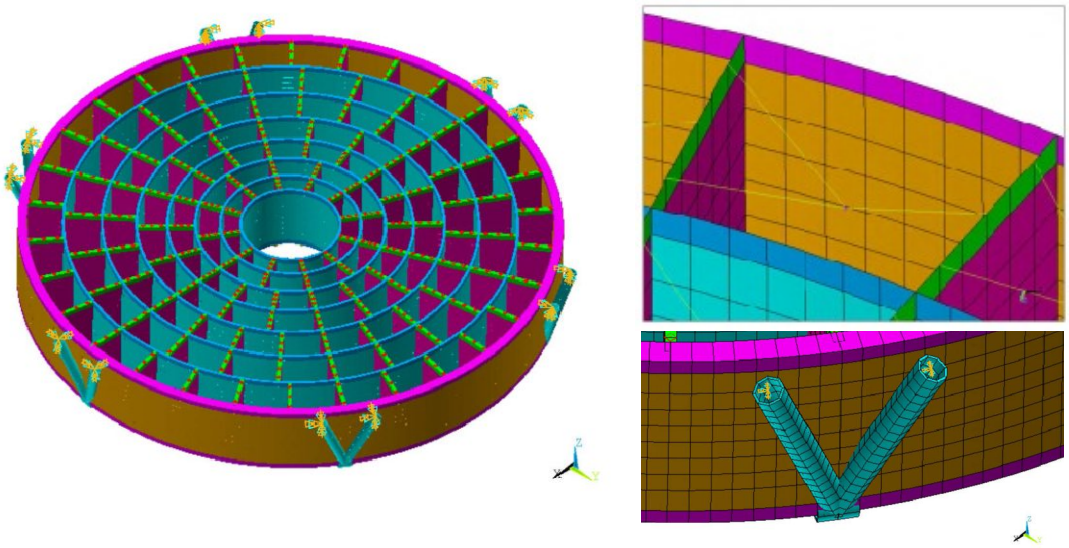

Figure 4 – FEM model (6 points mount with bibods)

Table 2 – Material and proprieties

Material	*Application*	*Density [kg/m^3]*	*E [MPa]*	*Poisson ratio*	*CTE [1/mK*10^{-6}]*	*Thermal conduct. [W/mK]*	*Yield strength [MPa]*	*Rupt. strength [MPa]*
CFRP	Structure	1600	65000	0.2	1.90	28	-	250
SiSiC	Mirror frames	3070	395000	0.17	3.00	120	-	350
Eagle XG	Mirror shells	2430	74800	0.238	3.55	1.09	-	-
Borofloat 33	Ribs	2200	57600	0.2	3.25	1.2	-	-
EP30-2	Glue	1400	2760	0.34	45	0.5	-	19
Stainless steel	Screws	7900	200000	0.3	16	15	185	500
Ti alloy	Screws, brackets	4930	105000	0.3	7.07	7.6	759	793
Invar	Brackets	8200	137000	0.29	1.50	12.8	240	440

2.2 EIGENFREQUENCIES

A trade-off has been performed for the different mounting conditions. In all cases the model is hardmounted at the corresponding interface nodes.

Table 3 - Fundamental eigenfrequencies (Hz) for different mounting configurations mode for the short version of MMs

	Req.	3-point mount	6-point mount
Rotational mode	N/A	52	52
Axial mode	>54	49	68
Lateral mode	30 - 35	33	74

The 3 points mount is quite critical for vibration during launch and it is not recommended.

2.3 DEFORMATION

The deformation of the structure under static loads is shown in the following figures. The deformation will be present during assembly and metrology on-ground but will become effective in-orbit after release of gravity. Due to the quasi-isostatic mounting of the mirror modules, the deformation of the structure will mainly result in rigid body movement of the mirror modules and consequently to alignment errors.
The results are summarizes in the following tables comparing the 3-point mount and the 6-point mount.

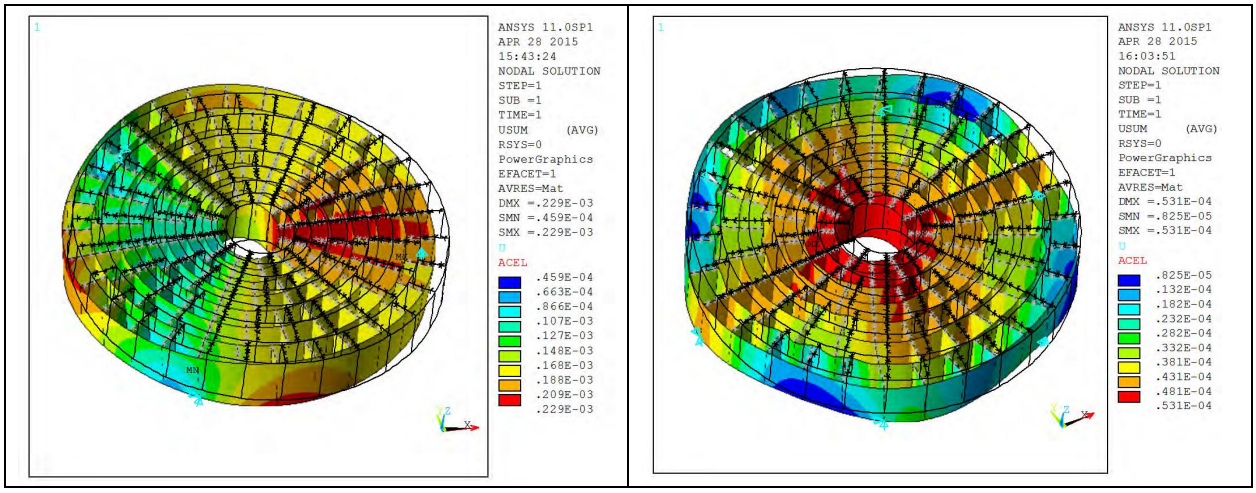

Figure 5 – Mirror assembly displacement due to lateral gravity for 3 points (left) and 6 points (right) constrained.

Table 4 - Displacement of the centre of gravity of the mirror modules under longitudinal gravity (Z)

Mounting	*Parameter*	*TX [µm]*	*TY [µm]*	*TZ [µm]*	*RX [µrad]*	*RY [µrad]*	*RZ [µrad]*
3-point	max	22.9	18.4	-32.7	131.7	117.4	73.2
	min	-14.2	-21.3	-117.8	-158.9	-167.8	-67.2
	PTV	37.1	39.6	85.1	290.6	285.2	140.4
6-point	max	11.8	11.5	-18.7	84.0	77.2	49.4
	min	-11.8	-11.5	-70.7	-84.0	-77.2	-14.5
	PTV	23.5	23.1	52.0	167.9	154.5	63.9

Table 5 - Displacement of the centre of gravity of the mirror modules under lateral gravity (X)

Mounting	*Parameter*	*TX [µm]*	*TY [µm]*	*TZ [µm]*	*RX [µrad]*	*RY [µrad]*	*RZ [µrad]*
3-point	max	-9.8	166.4	104.6	289.2	193.6	613.9
	min	-224.3	-132.7	-163.1	-429.4	-323.4	-566.0
	PTV	214.5	299.2	267.7	718.6	517.0	1179.9
6-point	max	-3.1	32.1	11.1	28.2	86.1	220.6
	min	-53.0	-6.5	-11.1	-127.9	-67.2	-220.6
	PTV	49.9	38.7	22.2	156.0	153.2	441.2

From the deformation points of view the 3-point mount is not recommended. In order to evaluate the PSF degradation, a ray-tracing has been performed for ring 5 (24 MMs), considering an HEW intrinsic contribution of each MM of 0.5". The mirror assembly deformation increase it to 6,4" for 3 supports and only 1.4" for 6 bipods case (Figure 6). The HEW increasing is due mostly to rotation of MMs around optical axis. Anyway the FEM model does not consider stiffness introduced by the MMs themselves and therefore it should overestimate the degradation. More detailed consideration will be studied in future activities.

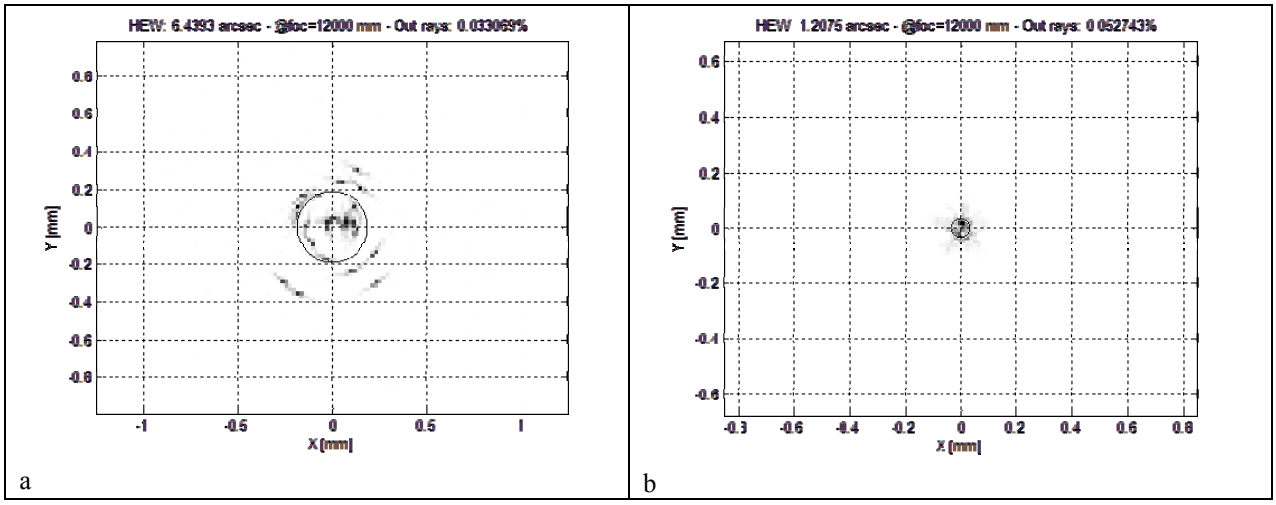

Figure 6 – PSF due to the petal distortion under lateral gravity (for simplicity only ring 5 is considered). HEW intrinsic contribution of each MM of 0.5". 3 points (a) and 6 bipods (b) cases.

2.4 STRESS

For preliminary sizing the following design loads are used:

- Axial 41 g
- Lateral 14 g

The resulting stresses are shown in the following table and figures. The peak stress is a local stress at the mounting points and it is not critical since the FEM does not contain any local reinforcements to account for interface areas as would be designed with suitable brackets to distribute the load over a larger area. The general stress level away from the mounting points is at a reasonable level.

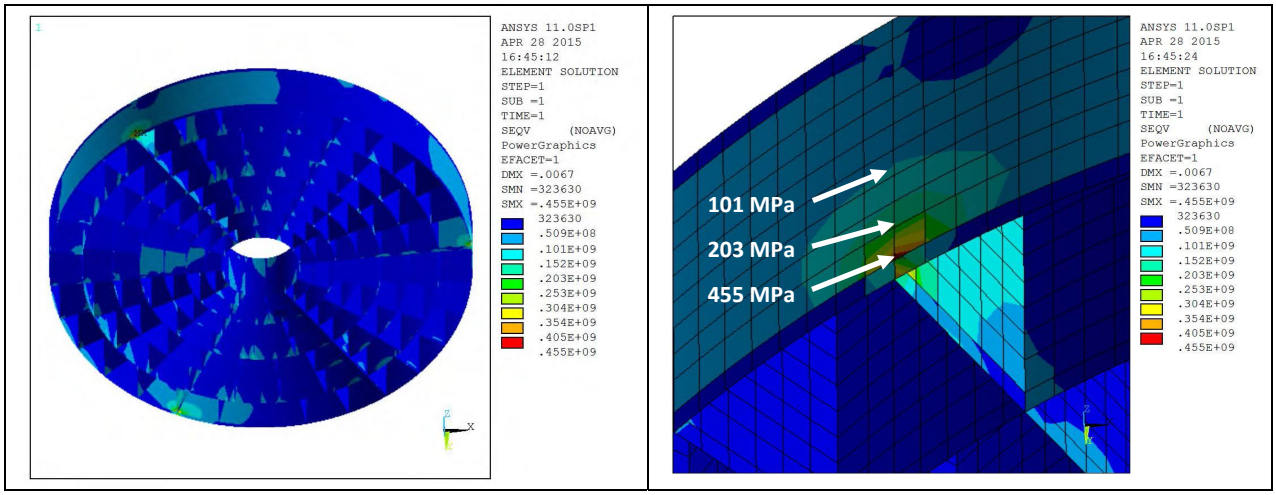

Figure 7 - Equivalent stress [Pa] at structure CFRP skins under 14g lateral (X) combined with 41g axial (Z), 3 supports

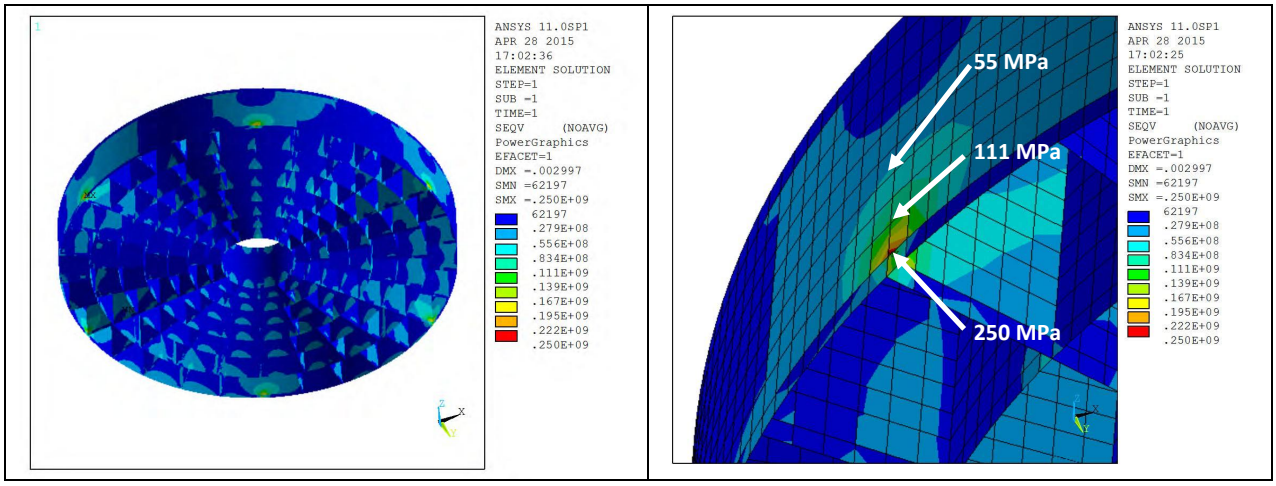

Figure 8 - Equivalent stress [Pa] at structure CFRP skins under 14g lateral (X) combined with 41g axial (Z), 6 supports

Table 6 – Maximum equivalent stress [MPa] in MMA structure

load	3 supports	6 supports	6 supports (with bipods)
Axial 1gZ	10.2	5.52	4.29 (structure); 1.83 (bipods)
Lateral 1gX	10.2	5.09	8.19 (structure); 9.03 (bipods)
41gZ, 14gX	455	250	N.A.
41gZ, 14gY	452	253	N.A.

The stress analysis suggests that for launch that at least 6 points are needed.

2.5 THERMAL ANALYSES

ATHENA is supposed to be operated at L2 in a stable thermal environment. One side is pointed towards the Sun (or Earth) with a small deviation only. For the mirror therefore only two conditions are relevant:

- Hold the temperature of the mirror module at 20°C with relatively low gradients and transients. This is the temperature at which the mirror is assembled and aligned. Any temperature change will degrade the accuracy (image errors and alignment errors) by thermo-elastic deformation. The required precision of the thermal control is to be defined in correlation with the overall error budget.
- In non-operational cases or failure cases the mirror must be held above a minimum admissible temperature to avoid degradation or rupture due thermo-elastic stress between parts with differential thermal expansion.

In both cases the mirror interface is maintained at the corresponding reference temperature by applying heater power on the MMs, while the open surfaces are radiating to deep space.
The mirror modules and X-ray baffles are modelled with separate planes, coupled by radiative and conductive results of the detailed thermal analysis (see section 3.4) and an effective emissivity to the environment of 0.4. Since the mirrors and baffles are modelled as planes, they show only the average temperature. The temperature gradients are determined with the detailed model. The bottom of the mirror assembly is facing a plane with T = 10 °C, simulating the optical bench and instrument platform of the telescope.
The results show that inside the mirror structure the temperature of azimuthal walls are characterized by a quite wide variation of temperature while in the radial walls the temperature is very near to 20°C because they are directly connected to the MMs. In order to hold the mirrors at 20°C a total heater power of about 1200 W is needed.
The temperature of the thermal baffle is about -20°C with a gradient of few degrees. The MLI temperature ranges from -153°C (opposite to the Sun) to 93°C (towards the Sun).

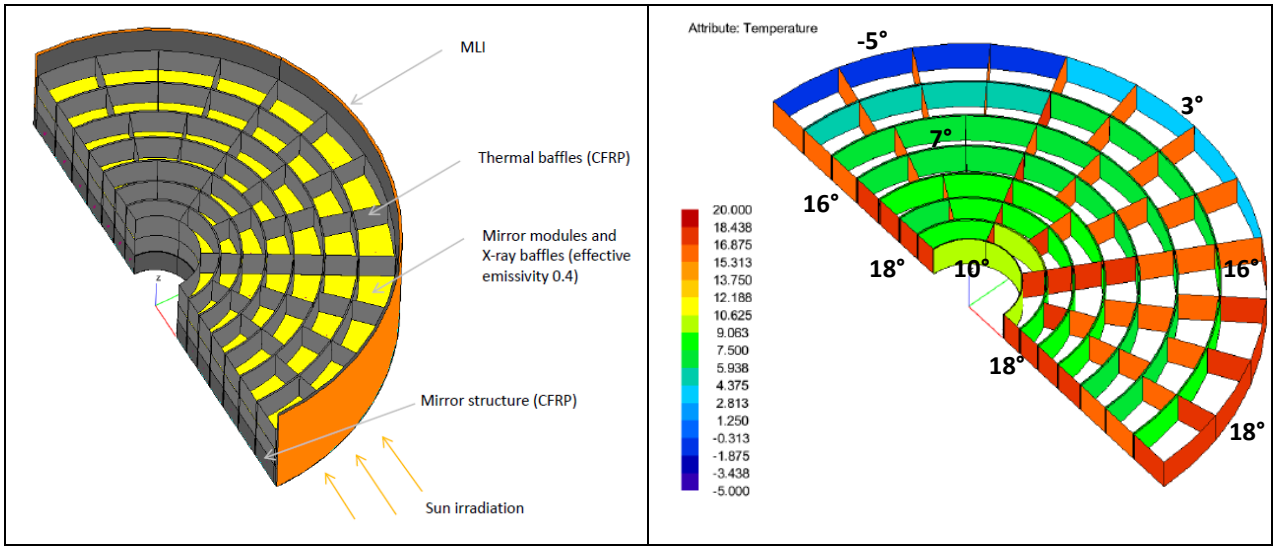

Figure 9 – Thermal model and resulting temperature field on the CFRP mirror structure. For symmetry reasons only half of the mirror assembly is modelled

For the survival condition the reference temperature is assumed 0°C and the resulting needed power is about 630W.

3. MIRROR MODULE

The proposed concept of a MM is shown in Figure 10: the interface with the petal is a three point connection in a plane perpendicular to the optical axis and approximatively positioned in the intersection plane. These points are connected with blades to a stiff supporting plate, named as mid-plane, made of SiSiC, where the optical shells are stacked in both sides.

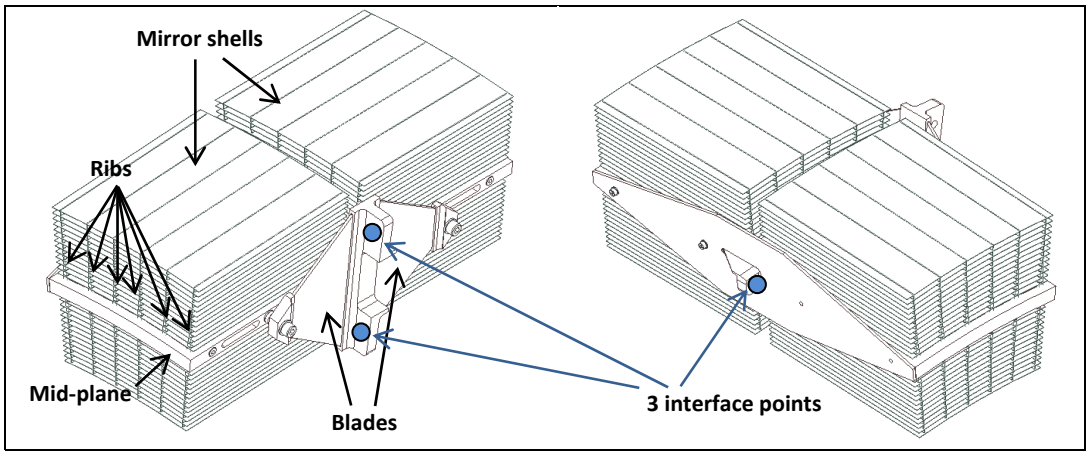

Figure 10 – Components of mirror module (ring n.5 for long version) without X-ray baffles

The two considered types of MM have glass foils with a different length in axial direction, 200mm for the long version and 100mm for the short version. In both cases the separation in the proximity of intersection plane is 20mm, needed for the integration process. It means that the distance between entrance plane and exit plane is respectively 420 mm and 220 mm. Another option is slumping the two surfaces concurrently with one foil. Some simulations have been performed in this configuration. The integration procedure is different, but the advantage is obtaining more stiffness in spite of a complexity in moulds realization. A prototype of this type has been recently developed[12] and also vibrated (Figure 11): sine dwell test (50g), random vibration and shock tests have been performed with success for all three directions.

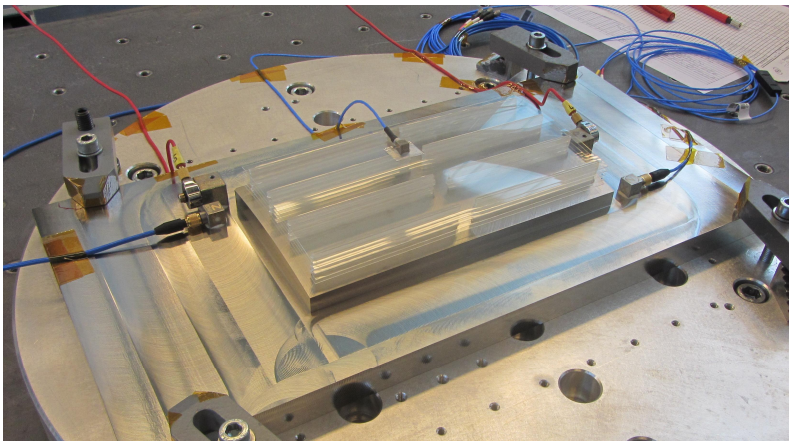

Figure 11 – vibration test of SGO prototype

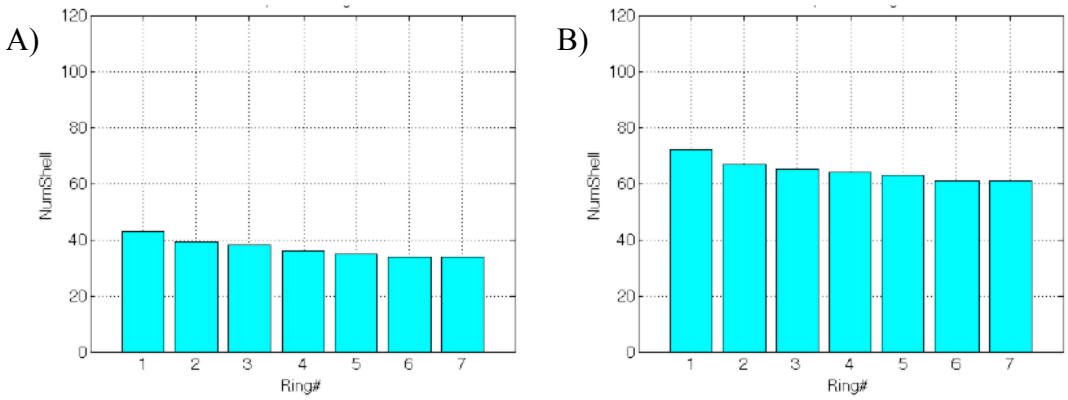

Figure 12 – number of shells pair for long (A) and short (B) version of MM.

The increasing number of shells for short version causes also a little decreasing of the collecting area, which has a major impact on the high energies because the shadowing due to the shell thickness (0.4mm) is more important for the inner diameters where the spacing from each optical shell is low. This effect can be seen in Table 7 where the effective area is presented.

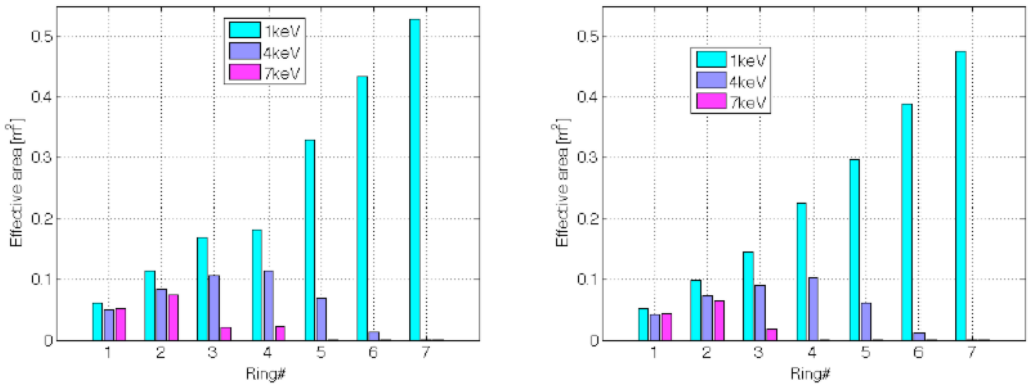

Figure 13 – effective area as function of the energy and diameter

Concerning the mass, for the short version it should be about 33% less than the long version, without any baffle. In Table 8 an estimation of the mass is shown together with the area/mass ratio, that is a more representative parameter for

a comparison between the two versions. If the weight of the petal and the baffle is considered the efficiency of short version is better than the long version while the behavior is opposite for the high energy.

Table 7 – Total effective area [m^2] with Pt+C coating

Energy	LONG	SHORT
1 keV	2.3519	2.1817
4 keV	0.4549	0.3767
7 keV	0.171	0.1263

Table 8 – Mass and efficiency estimation

	LONG	SHORT
MMs mass [kg]	881	582
Other mass (petal + baffles) [kg]	387	387
Total mass (no margin) [kg]	1268	969
Area/mass (1 keV) [cm^2/kg]	18.5	22.5
Area/mass (7 keV) [cm^2/kg]	1.34	1.30

3.1 X-RAY BAFFLE

Each MM is equipped with an X-ray baffle attached closest to the mirror module entrance plane. For the proposed thermal control, the X-ray baffle has to be made out of a conductive material (e.g. aluminium). There are two options (Figure 14):

- A stack of sieve plates similar to XMM[13] (lower mass).
- Cylindrical shells as used in eROSITA[14] (better thermal control). The X-ray baffle consists of shells forming a cylindrical extension of the X-ray mirrors.

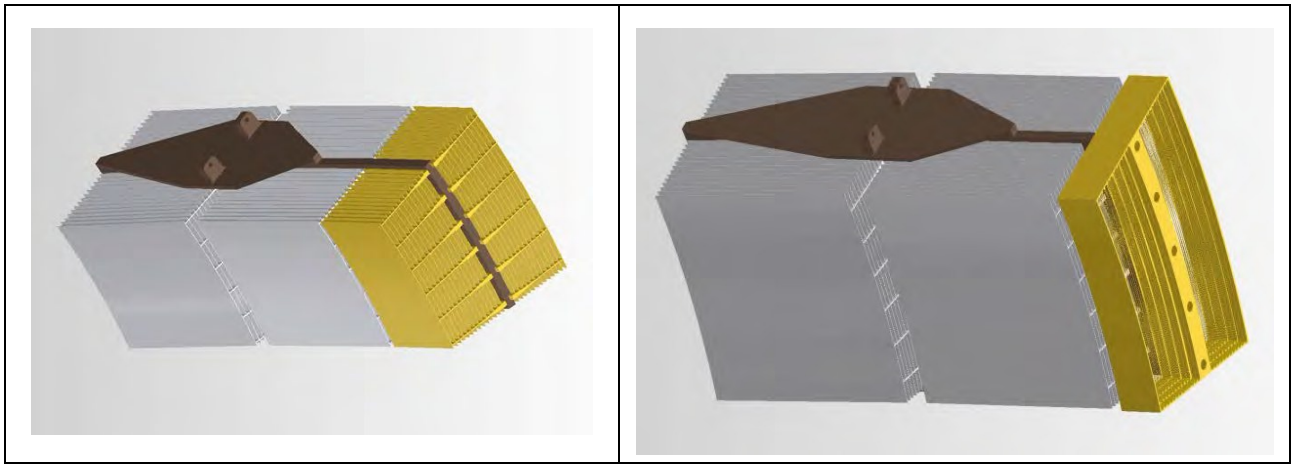

Figure 14 – two different concepts for X-ray baffle, cylindrical shell integrated together with the optical shells during integration (left) or sieve plates mounted after the optical shells integration (right).

An estimation of mass of all the MM baffles is 75 kg for sieve plates.

3.2 THERMOS-ELASTIC ANALYSIS

The deformation of the mirror shells under temperature change is calculated for a MM belong to ring 5 hard-mounted (isostatic). From this aspect, there is no significant reason to choose the long or the short module.

Table 9 – deformation of the mirror shells

Load case	HEW [arcsec]	
	400 mm	200 mm
Unif temp change +1°C	0.13”	0.07”
Radial gradient 1°C	1.45”	1.05”
Axial gradient 1°C	0.03”	0.93”

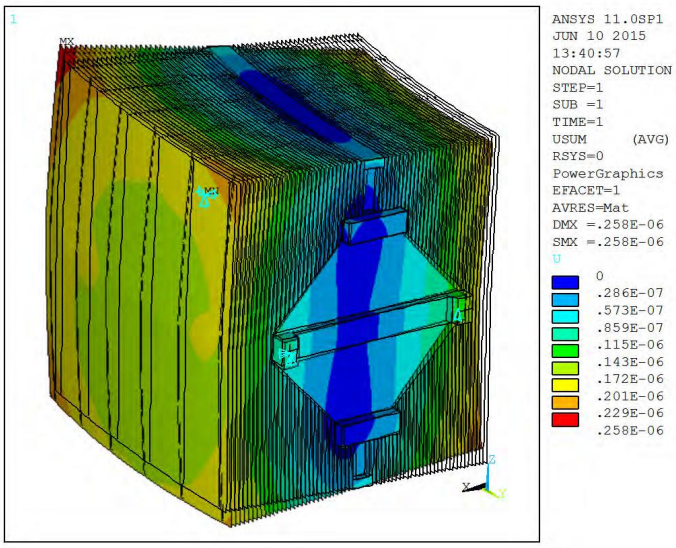

Figure 15 - Displacement [m] under radial temperature gradient (1°C) for the case with parabolic and hyperbolic surfaces slumped together

3.3 STRESS

For the MM, the considered loads for both long and short versions are 1g (applied to X, Y or Z direction) and a uniform temperature of 1°C (Table 10). For short MM in the table a hard-mounted fixation has been also shown as worst case. The real behaviour of interface points could be in between the isostatic and hard-mounted mode. For more detailed results on long MM refer to paper[9].

Table 10 – stress in the MM (ring5)

	1st principal stress (MPa)		Equivalent stress (MPa)	
	shells	ribs	Mid-Plane	Blade
	SHORT MM			
1gX	0.15	0.15	0.75	0.78
1gY	0.24	0.21	1.12	0.14
1gZ	0.03	0.05	0.61	0.97
dT+1°C isostatic mount	0.08	0.08	0.14	0.06
dT+1°C fix	0.08	0.08	0.55	1.81
	LONG MM			
1gX	0.17	0.16	2.19	0.14
1gY	0.13	0.19	1.32	0.59
1gZ	0.02	0.05	1.20	1.04
dT+1°C isostatic mount	0.03	0.08	0.32	0.07

3.4 THERMAL CONTROL

The thermal control has been analyzed for the case of MM of ring 5 integrated together with the X-ray baffle in the case of long shell by means of ESATAN. The thermal baffle passively limits the solid angle and therefore the heat loss to

space. Active temperature control of a single mirror module is realized by heaters on the inner and outermost shells of the mirrors and the X-ray baffle as well as on the upper part of the mid-plane. This gives a sufficient low temperature gradients of few degrees (Figure 16).

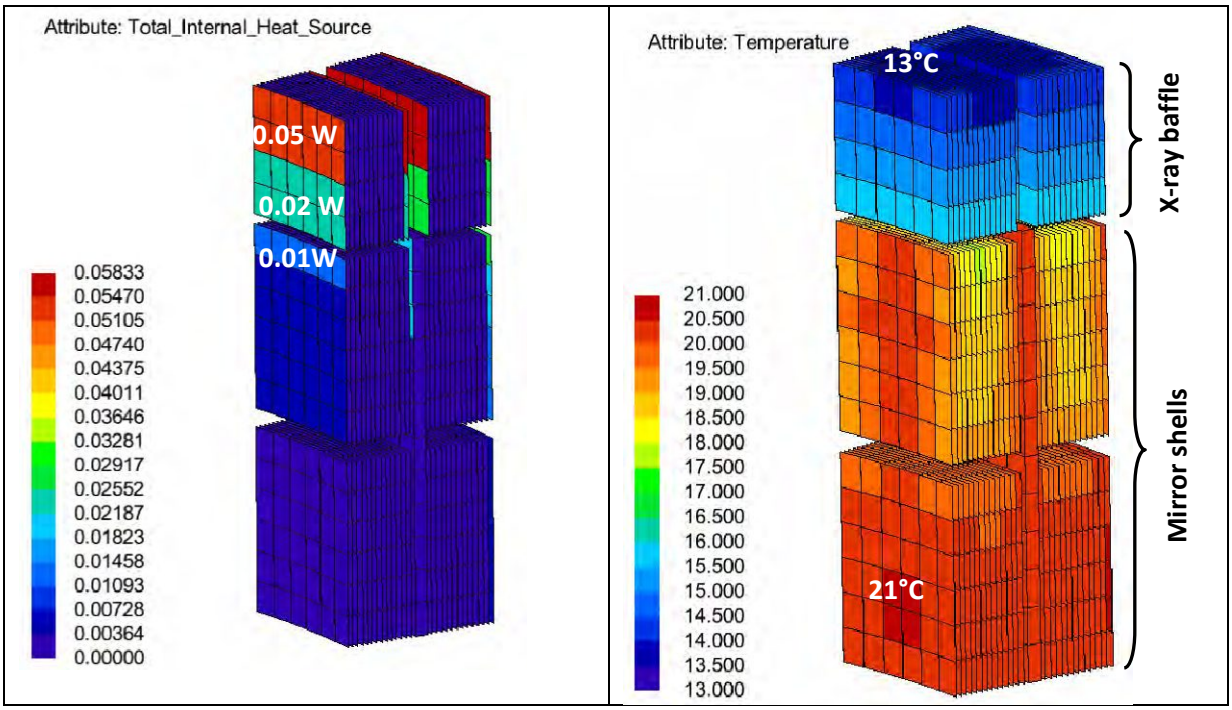

Figure 16 – Thermal analysis of MM of ring5. Thermal baffle and petal structure are not shown but taken into account in the calculation of the view factors.

4. CONCLUSION

The glass mirror shells for space represents an innovative technology for X-ray reflection and after NuSTAR success many proposed missions consider it as a good candidate for optics. The presented study shows a possible solution for the mirrors made with the SGO technology to implement into future large X-ray mission like Athena. The design tradeoff has been tailored considering the manufacturing capability in both module and assembly even if the developed prototypes does not yet fulfill the angular resolution required for an entire module. OAB, MPE and NASA are developing the slumping technology and good efforts have been made considering different integration methods. Actual reproducible results of shell in the required quality are as good as 10arcsec[15].

Extensive studies and tests have been performed to understand the structural characteristics of slumped glass and its capability to survive launch loads. This includes in particular vibration test, acoustic test and thermal cycling. With the current concept of stacked mirror shells a very robust solution has been found, fulfilling all needs for launch and orbit conditions. The partitioning in compact mirror modules facilitates precise integration of the high accuracy modules and alignment in a single mirror structure made in CFRP with high alignment stability and stiffness at low mass. The mass is about 1000 kg including MMs, petal, X-ray and thermal baffles. The minimum number of points for assembly fixation should be 6, but further analysis should be considered at a higher system level.

The same compact mirror modules have been optimized with respect to thermal control by active heating. Good thermal control performance can be achieved, although the glass has a very low thermal conductance. The design of the mirror modules tolerates some considerable thermal gradients which can be achieved by acceptable effort and the total heat power to maintain the optic to the reference temperature is about 1200W.

REFERENCES

[1] K. Nandra, X. Barcons, D. Barret, A. Fabian, J.W. den Herder, L. Piro, M. Watson, “Athena Mission proposal”, (2014)

[2] Maximilien J. Collon, Ramses Günther, Marcelo Ackermann, Rakesh Partapsing, Giuseppe Vacanti, Marco W. Beijersbergen, Marcos Bavdaz, Kotska Wallace, Eric Wille, et. al., "Design, Fabrication, and Characterization of Silicon Pore Optics for ATHENA/IXO", Proc. of SPIE Vol. 8147 81470D-1 (2011)

[3] B. Salmaso, S. Basso, C. Brizzolari, M. Civitani, M. Ghigo, G. Pareschi, D. Spiga, G. Tagliaferri, G. Vecchi, "Production of thin glass mirrors by hot slumping for X-ray telescopes: present process and ongoing development", Proc. of SPIE 9151-103 (2014)

[4] M. Ghigo, S. Basso, M. Bavdaz, et al., "Hot slumping glass technology for the grazing incidence optics of future missions, with particular reference to IXO", Proc. of SPIE Vol. 7732 77320C-1 (2010)

[5] M. Civitani, S. Basso, O. Citterio, P. Conconi, M. Ghigo, G. Pareschi, L. Proserpio, B. Salmaso, G. Sironi, D. Spiga, G. Tagliaferri, A. Zambra, F. Martelli, G. Parodi, P. Fumi, M. Tintori, D. Gallieni, M. Bavdaz, E. Wille, “Accurate integration of segmented x-ray optics using interfacing ribs”, Opt. Eng. 52(9), 091809-091809, (2013)

[6] A. Winter, E. Breunig, P. Friedrich, L. Proserpio, "Progress on indirect glass slumping for future x-ray telescope optics", Proc. of SPIE. Vol. 9144 91441C (2014)

[7] F.A. Harrison, S. Boggs, F.E. Christensen, W.W. Craig, C.J. Hailey and D. Stern, "The Nuclear Spectroscopic Telescope Array (NuSTAR)", Proc. SPIE 7732, (2010) 10.1117/12.858065

[8] M. Civitani, M. Ghigo, S. Basso, L. Proserpio, D. Spiga, B. Salmaso, G. Pareschi, G. Tagliaferri, V. Burwitz, G. D. Hartner, B. Menz, M. Bavdaz, E. Wille, "Direct hot slumping and accurate integration process to manufacture prototypal X-ray Optical Units made of glass", Proc. of SPIE Vol. 8861 886110-1 (2013)

[9] S. Basso, E. Buratti, M. Civitani, G. Pareschi, B. Salmaso, D. Spiga, M. Ghigo, G. Tagliaferri, J. Eder "A high resolution large x-ray mission based on thin glass: optomechanical design", Proc. of SPIE Vol. 9144, 91444C (2014)

[10] "Assessment of an X-Ray Telescope for the ESA Cosmic Vision Program (CDF Study Report) ", ATHENA-ESA-CDF-150 (A)

[11] P. Predehl, R. Andritschke, W. Becker, W. Bornemann, H. Bräuninger, H. Brunner, T. Boller, V. Burwitz, W. Burkert, et al., "eROSITA on SRG", Proc. of SPIE. Vol 9144 91441T (2014)

[12] L. Proserpio, E. Breunig, P. Friedrich, A. Winter, J. Eder, V. Burwitz, G. D. Hartner, B. Menz, M. Civitani, S. Basso, E. Buratti, "JIM: a Joined Integrated Module of glass X-ray optics for astronomical telescopes", Proc. of SPIE, 9603-33 (in press)

[13] D. de Chambure, R. Laine, K. van Katwijk, W. Ruehe, D. Schink, E. Hoelzle, Y. Gutierrez, et al., "X-ray baffle of the XMM telescope: development and results", Proc. SPIE. 3737, 396 (1999)

[14] P. Friedrich, C. Rohé, R. Gaida, J. Hartwig, F. Soller, H. Bräuninger, B. Budau, W. Burkert, V. Burwitz, J. Eder, G. Hartner, B. Menz, P. Predehl, "The eROSITA x-ray baffle", Proc. SPIE. 9144 91444R (2014)

[15] Ryan S. McClelland, Michael P. Biskach, Kai-Wing Chan, Rebecca A. Espina, Bruce R. Hohl, Elizabeth A. Matson, Timo T. Saha, William W. Zhang, "Design, construction, and testing of lightweight x-ray mirror modules", Proc. SPIE. 8861 88610O. (2013)